ELSEVIER

Thermochimica Acta 300 (1997) 67–82

thermochimica acta

Phonon dispersion treatment for the heat capacities of vitreous and crystalline phases

Edgar F. Westrum Jr.*

Department of Chemistry, University of Michigan, Ann Arbor MI 48109-1055, USA

Received 30 August 1996; accepted 14 November 1996

Abstract

Based upon the Barker and Martin treatment developed for the analysis of vitreous phases, an analysis of both polycrystalline and crystalline phases of various complexity is described. Primarily, cryogenic heat-capacity measurements and spectroscopic vibrational analysis are involved. Some history of the development of the phonon dispersion equations is incorporated. The applicability of the phonon velocity dispersion to polycrystalline and single-crystal copper are used as convenient examples to illustrate the application of the theory. They emphasize the complications occasioned by anisotropies in single crystals even in polycrystalline aggregates, where they are only partially obscured by the macroscopic isotropy of aggregates. Copper does involve the treatment of the electronic terms and demonstrates a competence of critical relevance to other types of crystalline and vitreous materials. © 1997 Elsevier Science B.V.

Keywords: Condensed matter; Glasses; Heat capacity; Phonon dispersion; Theoretical evaluation; Vibrational contributions

1. Historical overview

1.1. Introduction

The treatment of the vitreous state – once considered unacceptable for an equilibrium thermodynamics analysis – was pioneered in 1959 by Barber and Martin [1] in their interpretation of the deviation from Debye-like heat-capacity data results.

Over recent decades, glasses have been a favorite subject in our heat-capacity evaluations at the University of Michigan. As long ago as 1950, the silica glass, quartz, cristobalite, coesite and stishovite were all measured together with metamict, the intermediate density phases generated by nuclear pile radiation on both vitreous silica and quartz. All had the composition SiO_2, but great variation in mass density. Later, more than twenty polymeric vitreous macromolecular polymers and vitreous B_2O_3 were also examined. A number of alkali di- and tri-silicates were also treated and analyzed. Still more recently, we initiated measurements on nearly a score of selected binary and ternary alkali and alkaline-earth systems at Ann Arbor (1994 and 1995). Currently, a series of vitreous phases of ternary silicate oxides are underway.

Although all of these studies have enhanced our knowledge of the vitreous phase (e.g. a near Schottky representation of the remarkable glass-crystal difference, etc.), the definitive presentations have not yet

*Corresponding author. Tel: 1-313-764-7357; fax: 1-313-647-4865; e-mail: westrum@umich.edu.

PII S0040-6031(96)03122-X

been consummated. This document can only hint at the progress underway, while reviewing and correlating this important matter which is exciting enough to justify a preview.

As indicated, the measurements of low-temperature heat capacities, analyzed and interpreted, were begun in a comprehensive program in 1950–55 to determine experimentally and understand theoretically the distributions, $g(\nu)$, of thermally excited modes of motion as a function of their frequencies, ν. Such functions, conventionally represented by $g(\nu)$ vs. ν, are implicit in all thermal, mechanical, and optical properties of elastic solids and, in principle, can be found by inversion of heat capacities as functions of Kelvin temperature T, volume per mole of oscillators V, and pressure P. Conversely, when $g(\nu)$ vs. ν is known, all physical properties of elastic solids, can, in principle, be formulated as functions of it.

In general, $g(\nu)$ comprises two classes of modes which must be distinguished because their frequencies are functions of distinctly different parameters of elastic solids: (1) acoustic modes of frequency $\nu_a = \nu(W_p)$, where $W_p(\nu_a)$ is the phase velocity in at least two polarizations p_a – over macroscopic distances in a solid defined by its macroscopic elastic constants c_{ij} and mass density ρ; and (2) optic modes of frequency $\nu_o = (f_i/m_i)^{1/2}$, where the f_i are force constants constraining the motion of atomic masses m_i and densities of atoms specified by the subscript 'i'. Optic modes are localized in stationary distributions of atomic masses m_i and, therefore, do not travel or contribute to the thermal conductivity, κ, which depends exclusively on acoustic modes.

To facilitate distinction of optic from acoustic modes, our measurements of C_V (T) were complemented by correlating determination of IR- and Raman-spectra of optic modes (ν_0) to be compared with C_V (T), which is a function of all frequencies, both ν_a and ν_o.

Our 1950–55 heat-capacity measurements on vitreous silica were the first ever at liquid helium temperatures, and they appeared so anomalous with respect to generally accepted interpretive theory that no analyses of it could be made until an appropriate analytical formula for the acoustic component of C_V vs. T could be derived as a function of $g_a(\nu, \nu_a^*)$, where ν_a^* is a limiting frequency defined by parameters of geometric arrangements of atoms in the solid. Such a formula was derived from first principles and published by Barber and Martin [1], and represents the foundation of this terse presentation. Meanwhile, our measurements on alkali silicate glasses and crystals were completed and measurements on vitreous silica up to $T \ll 4.5$ K were initiated by others who were convinced that the expected linearity of C_V vs. T^3 would be found at T sufficiently near 0 K. Such expectations were more justified in silica glass, because of its perfect isotropy, than in quartz where it was immediately evident in our data, regardless of significant anisotropy; but the T^3-law is not found in glasses even at $T < 0.1$ K – a fact that justified our immediate attention to refinement of relevant theory. Indeed, vitreous silica has heat capacities at $T < 1$ K about three orders of magnitude higher than crystalline quartz.

1.2. Derivation of the dispersion formulas

The necessary refinements of conventional Debye functions [2] for $g(\nu)$ vs. ν and $C_V(T)$ were easily perceived and readily formulated. The Debye functions were known by Debye himself to be crude approximations, because they were simplified by the assumption that acoustic wave velocity is independent of frequency, whereas W_p in both transverse and longitudinal polarization is ν-dependent. As will be shown, they can be improved to fit essentially within experimental uncertainties by introducing $W(\nu)$ vs. ν_a in place of Debye's constant $W(0)$; i.e. by representing velocity dispersion in $g_0(\nu, \nu_a^*)$ vs. ν. Such dispersion formulas were derived and published by Schrödinger [3], but the dramatic improvement in them has not been appreciated and they have been so neglected and underappreciated by reviewers and monograph writers that they have been rederived and evaluated by Barber and Martin [1] independently of Schrödinger, and again by Kieffer [4]. Such long neglect and repeated rediscoveries of the dispersion formulas – in spite of their quite obvious and self-evident advantages and the cogent logic of his derivation – is a problem to be understood before proceeding further. This text is intended to deter additional independent rediscoveries and unjustifiable detractions in the light of the persistence noted.

Derivation of the dispersion formulas (Barber and Martin, 1959) follows from Brillouin's [5]

fundamental description of wave propagation. Brillouin, Schrödinger's contemporary, certainly influenced him – as well as us. Both men were renowned scholars in wave mechanics and their prestige should have inspired more consideration of the dispersion formulas than was accorded them. Failure to do so is evidently due, in part, to at least one faulty review, but in greater part to circumstances beyond control or comprehension of reviewers.

1.2.1. Blackman and de Launay

Two comprehensive reviews were available to us during planning of our project: those of Blackman [6] and of de Launay [7]. Blackman [6] reviews not only his many earlier papers, but evaluates a dispersion formula (Eq. (5.8) in Ref. [6]):

$$\rho(\nu) = \frac{72N^3}{(2\pi)^3} \frac{\arcsin(\nu/\nu_0)^2}{(\nu_0^2 - \nu^2)^{1/2}}$$

similar to Schrödinger's, for which he cites Schrödinger's reference to an earlier paper by Born and von Kármán [8], where ν_0 is the limiting frequency (identified here as ν_a^*). This formula differs from Eq. (13) of Barber and Martin [1], where the arcsine is squared instead of its argument (ν/ν_0). The latter is in error and may explain Blackman's [6] ill-informed criticism: "There is little doubt that the Born–von Kármán function gives a less good fit with experimental data than the Debye function. It suffers further from a much less obvious derivation, nor does it link the specific heat data with elastic data of the solid. It is therefore not surprising that the theory should have attracted less attention than the Debye theory, though it is astonishing that this has occurred without any critical investigation."

Every statement in this quotation raises a serious question. First, replacement of the most suspect approximation in Debye's theory with more cogent assumptions should improve its conformance to experimental data. Failure to do so obviously indicates error in the derivation or in the experimental data and should be corrected rather than rejecting the more cogent theory. Second, our dispersion derivation is more obvious, rather than *less*, compared to Debye's approximation and it does "*link the specific heat data with elastic data*" more rigorously and with fewer arbitrary simplifying assumptions. Third, if he thinks "it is astonishing that this has occurred without any critical investigation," Blackman should make the critical investigation needed to support his contention. We did that and are led to firmly contradict his conclusions.

Most of the error in Blackman's judgments – cited here – arise from misapplication of his Eq. (5.8), despite the already noted error. Referring to it he writes, "The heat capacity function for the solid then depends on only one parameter $\theta_0 = h\nu_0/k$ in the form θ_0/T, where θ_0/T has to be chosen empirically." An adequately "critical investigation" would have shown that no solid can be accurately represented by "only one... θ_0/T." At least two θ_0's, representing transverse (θ_t) and longitudinal $(\theta_l > \theta_t)$, must be used and the effective mean θ_{tl} of these can be constant only at $T <\sim \theta_{tl}/50$ – much lower than the T between 22.8 and 86 K considered by Blackman [6] (cf. his Table 3, p. 334). In this range, θ_{tl} *increases* with T contrary to his calculations of θ_D, which decrease from 244 K at 22.8–215 K at 86 K. It will be shown later, that this surprising trend of θ_{tl} (T) is implicit in the analytical dispersion formula found first by Schrödinger [3], then rediscovered by Barber and Martin [1] and by Kieffer [4].

Criticism of Blackman, however, must be tempered by the fact that when he wrote his review, accurate experimental data at temperatures sufficiently low to verify the dispersion formulas were non-existent. Furthermore, tables of C_V vs. θ/T were first published by Barber and Martin [1] and Eq. (13) and (15) of that text could be verified only recently – 25 years after their publication.

Both Blackman and de Launay consider the ν-dependence of acoustic wave velocities and, after reviewing the relevant – but inadequate – experimental C_V (T) data available to them, both favor the conventional Debye formulas in which acoustic wave velocities are assumed constant – independent of ν, although the real limit $\nu_a^* = (2/\pi)\nu_D$ was common knowledge. The obvious error factors in ν_D, $(2/\pi = 0.6366)$, and in $C_V(\theta_D)$, $[(2/\pi)^3 = 0.2580]$ were tolerated for mathematical tractability, and ad hoc modifications of Debye's formulas were made to correct for them. De Launay's elaborations of Debye's formulas were the more rigorous and analytical in principle, but were derived for specific body-centered, face-centered, and diamondoid cubic

lattices and cannot be generalized for application to glasses wherein the detailed parameters of atomic lattices involved are intrinsically indeterminable, and cannot be inferred from experimental C_V vs. T data in any case. Furthermore, they are unnecessarily complicated and inconvenient. As will be shown, the dispersion formulas are much easier to modify for specific cases than are Debye's formulas because they are vastly more accurate generalizations.

Conventional inversion of $C_V(T)$ functions employs Debye's heat capacity function of a single $\theta_D = hV_D/k$ as an idealized reference function in which θ_D is constant for $0 > \nu < \nu_D$ and for all T. Experimental values of $C_V(T)$ can be represented by deviations of θ_{app} from the ideal constant value of θ_D calculated from elastic constants c_{ij} and mass density ρ of the solid, where θ_{app} is the 'apparent' value of θ_D required in the Debye function to make it match the experimental C_V at every experimental temperature T. Obviously a plot of $\theta_{app}(T)$ can represent any solid as accurately as $C_V(T)$ can be measured and the plot inferred from $\nu_{app} = h\theta_{app}/k$ characterizes a solid nearly as well as do its Raman- and IR-spectra. Even so, its interpretation is obscure and misleading, because it represents deviations from a function that is irrelevant to any solid except as $\nu \rightarrow 0$. Indeed, any nominal function of $\theta(T)$ can serve as a reference function regardless of error in it and will yield a characteristic θ_{app} vs. T plot. Eq. (15) of Barber and Martin [1] serves this purpose but because it conforms so exactly to the behavior of real solids, deviations from it are relatively small and their implications regarding density of states are immediately apparent. Its use in this way can be demonstrated on selected simple crystals and its application to glasses better understood.

1.2.2. Tarassov's development

We were not the first to seek structural information from $C_p(T)$ of glasses. Between 1945 and 1957 – before any data suitable for such inferences was available – Tarassov published a series of papers in which he claimed to show that "specific heat functions for chain-like structures" could be found in "temperature dependence of the specific heat of vitreous B_2O_3," for example, and that similar evidence of layered structures could be found in certain silicate and borate glasses. Several of his papers are reviewed collectively and expanded into a book [9]. Some of his papers were available to us during planning of our measurements on silica glass but were of no value to us because the data analyzed in them were, in every case, for temperatures so high that essentially all optic as well as acoustic modes were excited and no isolation of acoustic modes from overwhelming densities of optic modes was conceivable. The data on vitreous boron anhydride, for example, between 68.6 K and 169.4 K, where he found quite precise linearity of C_V vs. T in accord with his ardent – but unjustifiable – expectations. Linear extrapolation of this data (from 68 K to 0 K) even yields $C_V = 0$ at $T = 0$ as his hypothesis required; but such linearity is not in accord with dispersion formulas for such high temperatures. Some linearity at such temperatures is *always* expected near unavoidable inversions of slope in $C_V(T)$ curves regardless of chain-like or layer-like elements of structure.

In the first part of his book, Tarassov reviews derivations of dispersion formulas for distributions of states in one, two, and three dimensions, citing Born and von Kármán (1913) [8] and Blackman (1955) [6]; but, like his predecessors, he provides no numerical values of heat capacity vs. θ/T for any of these dispersion functions. Evidently, he derived them only to show that they reduce to Debye-like functions of $(T/\theta_1)^1$, $(T/\theta_2)^2$, and $(T/\theta_3)^3$ as $T \rightarrow 0$, where dispersion effects are negligible. Then, knowing that such functions can exist at *some* temperature, he looks for them at *any* temperature and assumes *any* value of θ_1 or θ_2 required to fit the data. In crystalline B_2O_3, for example, his values of θ_2 for 'layer structures' vary from 943 K at $T = 104.82$ to 1320 K at 271.1 K and $\theta_{1(0.2)}$ for 'chain-like structures' varies from 1556 K at $T = 104.12$ K to 1869 K at 296.00 K. These values are absurd even for optic modes dominant at such temperatures, and more absurd for acoustic modes which could be observed only at $T < 15$ K.

In 1955, when our data on vitreous silica and cristobalite were first available, Dank and Barber (1955) [10] showed that both glass and crystal of identical composition have remarkably similar $C_V(T)$ curves, and both conform quantitatively to an ad hoc modification of a formula in T^2 and T^3, originally proposed by Tarassov [9]. Because the dominant term in that formula was $C_2(\theta_2/T)$, representing a two-dimensional distribution of modes and,

by assuming mass units of Si_3O_6 as would be appropriate for quartz, we could infer plausible values of $\nu_2^* = 115\,cm^{-1}$ and $117\,cm^{-1}$ in vitreous silica stabilized at 1070 and 1300°C, respectively, and $113\,cm^{-1}$ for cristobalite from slopes of C_V vs. C^2; we could say that "These new observations...suggest the existence at low temperatures of highly anisotropic structures for cristobalite and vitreous silica..." In the same sentence, however, we cautioned that both of these solids "have been regarded as isotropic on the basis of X-ray studies and the macroscopic isotropy of various physical properties." Our latest analyses will show that these earliest results were entirely fortuitous, however provocative they seemed then.

Years later, Tarassov (1967) [11] discussed our data on silica. As could have been predicted from his earlier book [9], he found evidence that the 'chain model' applies to the thermal capacity of vitreous silica up to 900 K. Evidently, it did not occur to him that any model applies equally well to any material at 900 K because heat capacities approach their classical (Dulong and Petit) limit at $T \ll 900\,K$, where they tend to become constant and completely independent of structural details. His curve-fitting exercises without due account of velocity dispersion cannot lead to credible results; but, because they have been published and can mislead others, it was necessary to 'describe' them before a more germane procedure could be presented – the ultimate purpose of the following text.

2. The preeminence of velocity dispersion

Contrary to the opinions of the reviewers, Blackman [6] and de Launay [7], and to conventional practice favored by them and by most textbook writers, analyses of experimental C_V vs. T curves to find distributions of acoustic modes is more reliably, and more conveniently done by inversion of heat-capacity functions of velocity dispersion than by inversion of Debye functions. This is self-evident, because velocity dispersion is a sensitive function of structural parameters; all of these are neglected or obscured in complicated effective averages in Debye's formulas. Such reliability and convenience is not realized without reliable formulas for acoustic components of C_V vs. T and tested procedures for applying them. Because conventional practice does not prescribe such formulas or procedures, they are prescribed as follows: first, the formulas for acoustic components of C_V and their inversions to values of $\theta_{app} = h\nu^*/k$ are required to make the functions match experimental values of C_V for all temperatures measured. The bar in $\overline{\nu}^*$ indicates that $\theta_{app}(T)$ always represents an effective mean of two or more quite different limiting frequencies; all of these must be specified in formulas for $\theta_{app}(T)$.

Admittedly, the form of Schrödinger's equation was mathematically difficult to integrate, but it is correct. Some reviewers and textbook authors have cited Schrödinger's dispersion equation among their references but few – if any – have discussed it adequately and virtually none have published tables of its heat-capacity integral, comparable to the ubiquitous Debye function tables.

It is interesting to note in passing that Debye's unmentioned neglect (simplification) of dispersion has fueled, in recent years, not only the Barber and Martin [1] treatment of glasses, but the Kieffer [4,12] treatment of mineral thermodynamics as well, and the Komada and Westrum [13,15] or Komada [14] development of a single parametric phonon dispersion approach for evaluation of the temperature dependence of C_V for lattice contribution in material phases.

In order to demonstrate the approach for two distinguishable phases I have elected to choose a metallic rather than a vitreous phase for an illustration. A vitreous phase had been tersely discussed [1], and to contrast such a phase with a crystalline one of the same composition would have taken much more space here. Moreover, the comparison of polycrystallne copper with single-crystal copper (said to be 'indistinguishable' by the person who measured their heat capacities) provides an opportunity to treat the electronic contribution also. The treatment applied as well to diamond, tungsten, aluminum, sodium chloride, etc. is also shown to be of wide utility in dealing with the thermophysics of phases other than the vitreous one.

It would, however, have been logical here to discuss the nature of the frequently misunderstood primitive cell both for the vitreous and metallic phase, but space does not permit that.

3. Treatment of copper metal

Copper ($fcc, f = 1$, isotropy index – 0.317) is chosen to model the effects of anisotropy on acoustic

Table 1
Experimental C_V vs. T and elastic constants, c_{ij}, s_{ij}, vs. T in crystalline and polycrystalline copper

Relevant physical properties
Gram formula mass (GFM)=63.54
Mass density at $T = 0, \rho = 9.0305\,g\,cm^{-3}$.
Number density of atoms, $N/V = 8.553 \times 10^{22}\,cm^{-3}$

C_V vs. T: Shown as a continuous function of T in the 0–300 K range

C_V vs. T	θD (K)	$\bar{\theta}(0) = 2\theta_D/\pi$ (K)	$10^5\gamma/3R$	Reference
1.3–20 K	346.3	220.5	2.790	[16]
1.0–30 K	343.7	218.8±0.6	2.763	[17]
0.3–3 K	347.7±0.8 [a]	221.4±0.5	2.764	[18]
Single crystal				
0.3–3 K	346.6±1.4 [a]	220.7±0.9		[19]
Polycrystalline				
20–300 K				[20]
Polycrystalline				

[a] Martin [19] concludes "that, within experimental accuracy, there is no difference in the specific heat of pure single-crystal and pure polycrystalline copper." (p. 1254). Differences of this magnitude are significant in Eq. (12) of [1] which may indicate what differences should be expected and for what reasons.
Comment: Phillips [21], in his review, Low Temperature Heat Capacity of Metals, cites 26 independent values of θ_D for copper. Three of these, 371.7, 338.9, and 327.0, are extreme and can be rejected as outliers. The remaining 23 are between 342.0 and 345.6 and randomly distributed around his selected value 344.5. The spread (larger than experimental uncertainties) must be explained. Experimental values of $\theta(T)$ inferred from C_V vs. T measurements cited are represented graphically in Fig. 1 where the limiting values of $\bar{\theta}(0)$ and $\bar{\bar{\theta}}$ are labeled. The highest value of $\bar{\theta}(0)$, 221.4 K, is Martin's value for a single crystal. This is the highest reliable value reported in the literature, while 218 is the lowest reliable value. The intermediate value, 220.5 is the mean of Wycherley's data below 4 K adjusted to be consistent with $\gamma/3R = 2.795 \times 10^{-5}$ as shown in Fig. 2. Wycherley's values (γ=6.696 mJ (g at)$^{-1}$ K^{-2}, θ_D=346 K) had to be extended to four significant figures to be mutually consistent with $\bar{\theta}(0)$ in plots of $\ln(C_V - \gamma T)/3RT^3$ vs. ln T as shown in Fig. 2 which represents his primary data to five significant figures. Methods of interpretation used here allow greater precision than he could claim by conventional Debye methods.
The upper limit, $\bar{\theta}(4/\pi)^{1/3} = \sim 280$, is less accurately determined graphically because apparent values of $\bar{\theta}(T)$ are relatively insensitive to T near θ_l. Preliminary values within $\sim \pm 2\%$ are easily adjusted within $\sim\pm 0.5\%$ by iterations through Eq. (12) of Ref. [1] to be consistent with $\bar{\theta}(0)$ to four significant figures.

spectra in otherwise simple monatomic primitive lattices, because it is most adequately characterized experimentally for T from 0 to 300 K as required for comprehensive validation of Barber and Martin's [1] Eq. (12). The experimental data required are presented in Table 1 which includes selected values of C_V vs. T along with derived values of θ_D and $\bar{\theta}(0) = 2\theta_D/\pi$. The experimental $\theta(T)$ vs. ln T is presented in Fig. 1 so as to display the extreme values, at $\theta(0)$ and $\bar{\bar{\theta}}$ at $T > \theta_l$, and for detailed comparison with calculated values from Eq. (12) in Ref. [1] over the range $\Delta\theta = \theta - \theta(0)$. The corresponding $\ln(C_V/3RT^3)$ vs. ln T are presented in Fig. 2. Formulas for elastic constants c_{ij} as functions of T, as derived from literature tables are assembled in Table 2 and represented graphically in Fig. 2 where the bulk modulus of the conduction electron gas, $\kappa_e(T)$, is correlated with lattice bulk moduli, κ_L, and rigidity moduli, G_L, both as functions of T.

3.1. Critical effects of anisotropy in copper

The experimental C_V vs. T data for copper display several critical consequences of anisotropy in metals, some of which are inadequately understood and must be clarified in this text.

(a) The range of variation in $\theta(T)$ from $T = 0$ to $T = \bar{\bar{\theta}}(4/\pi)^{1/3}$ is quite large in copper as shown in Fig. 1, where $\Delta\theta \approx 60$ K. In large single crystals, where all acoustic modes can be accounted for as families of parallel plane waves, $\bar{\theta}(0)$, $\bar{\bar{\theta}}$, and $\Delta\theta$ are functions of elastic constants c_{ij} (in stress) and s_{ij} (in strain) which are conventionally assumed to be independent of T over ranges of interest when the $C_P - C_V$ correction to constant volume is applied. In this simple case, the bulk moduli of the lattice, κ_L, are increased by the relatively large bulk modulus κ_e of the conducting 'electron gas' enmeshed under pressure in the crystal lattice of atoms as explained in de Launay's

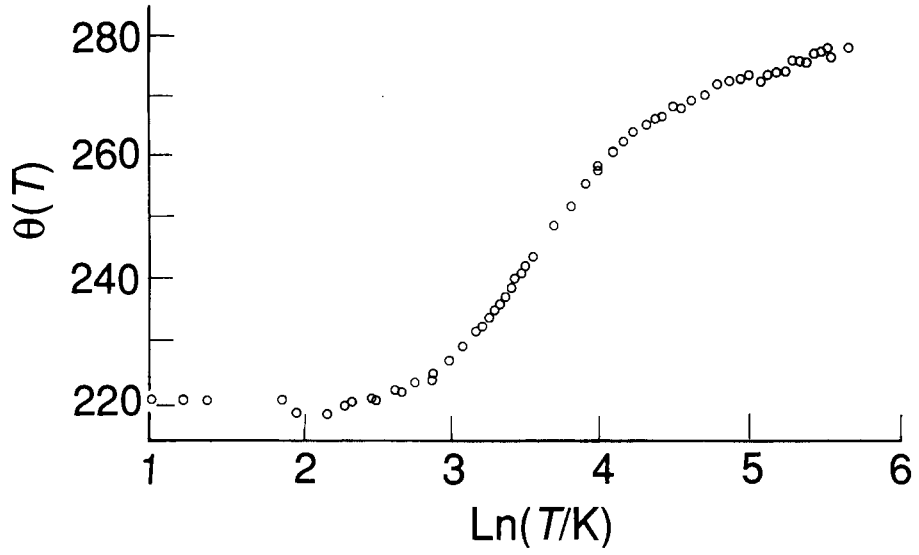

Fig. 1. Apparent $\theta(T)$ vs. $\ln(T/K)$ for copper. $\bar{\theta} = 221.4\,K$, single crystal; $\bar{\theta} = 220.7\,K$, polycrystal; $\bar{\theta} = 218.0\,K$ lowest reliable value. $\bar{\bar{\theta}}(4/\pi)^{1/3} \approx 180\,K$. $\Delta\theta \approx 60\,K$.

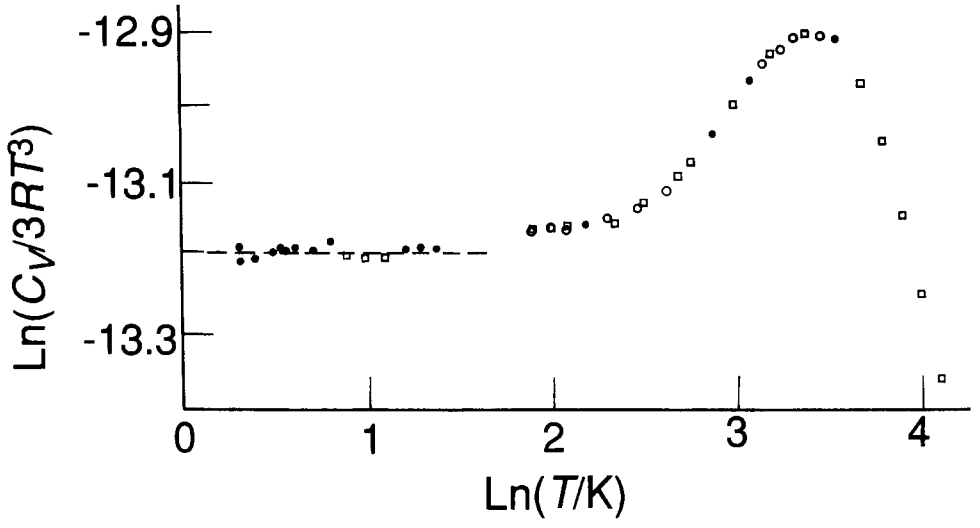

Fig. 2. Ln $(C_V/3RT^3)$ vs. ln (T) for polycrystalline and single crystal copper. • – Wycherly [16] $\bar{\theta}(0) = 220.5$, intercept=−13.189; ○ – Cetus et al. [17]; □ – Martin [20], single crystal; $\bar{\theta}(0)$ intercept=−13.199, and Martin [19], polycrystalline, $\bar{\theta}(0)$ intercept=−13.189.

review [7]. In small crystals constrained to fixed positions in polycrystalline aggregates, complications due to constraints and deforming forces from contiguous, randomly oriented crystals are added to the isotropic pressure effects of the electron gas. Moreover, in this case the rigidity moduli, G, can also be modified by κ_e as a measure of deformation strain. They are not independent of κ_e, as de Launay could assume for strain-free single crystals:

(b) Complications considered in (a) imply that polycrystalline aggregates differ significantly from single crystals – contrary to Martin's conclusion from experimental evidence "that, within experimental accuracy, there is no difference..." (p. 1254 in

Table 2
Temperature dependence of mode distribution in polycrystalline copper

θ (lmn) at $T \equiv 0$	As a linear function of $T > 100$		Eq.
$\theta_l(100)$: 368.9	$371-0.0322T$, $T < 600$	$378-0.0400T$, $T > 600$	(5.1)
$\theta_l(110)$: 423.5	$425-0.0333T$, $T < 400$	$429-0.0444T$, $T > 400$	(5.2)
$\theta_l(111)$: 440.2	$442-0.0333T$, $T < 400$	$448-0.0500T$, $T > 400$	(5.3)
$\theta_{le}(100)$: 411.5	$413-0.0344T$, $T < 400$	$417-0.0322T$, $T > 400$	(5.4)
$\theta_{le}(110)$: 442.8	$445-0.0278T$, $T < 400$	$450-0.0389T$, $T > 400$	(5.5)
$\theta_{le}(111)$: 452.7	$454-0.0311T$, $T < 400$	$459-0.0433T$, $T > 400$	(5.6)
$\theta_{t1}(100)$: 251.3	$254-0.0378T$, $T > 100$		(5.7)
$\theta_{t2}(100)$: 257.3	$254-0.0378T$, $T > 100$		(5.8)
$\theta_{t1}(110)$: 251.3	$254-0.0378T$, $T > 100$		(5.9)
$\theta_{t2}(110)$: 140.7	$144-0.0311T$, $T > 100$		(5.10)
$\theta_{t1}(111)$: 185.0	$188-0.0311T$, $T > 100$		(5.11)
$\theta_{t2}(111)$: 185.0	$188-0.0311T$, $T > 100$		(5.12)
$\theta_e(100)$: 182.6	$181+0.0193T$, $T > 100$		(5.13)
$\theta_e(110)$: 182.6	$181+0.0193T$, $T > 100$		(5.14)
$\theta_e(111)$: 182.6	$181+0.0193T$, $T > 100$		(5.15)

Comments:(1) All coefficients of T are negative *except* in equations for θ_e(lmn) vs. T. This is important because all additive combinations of θ_e with lattice modes makes their T-dependence negligible. (2) Transverse (111) modes are nearly equivalent to θ_e at $T = 0$. Their difference, $7-0.0504T$, is zero when $T \rightarrow 139$ K which approximates $\theta_{t2}(110) = 140.7$. This suggests that θ_e may augment $\theta_{t2}(110)$, $\theta_{t1}(111)$, and $\theta_{t2}(111)$ in strained copper crystals. It may also combine with $\theta_l = 251.3$ to create a deformation mode at $173-0.0571T$.

[20]). That conclusion was inferred from measurements below 3 K where velocity dispersion is negligible. It does not apply at $T > 3K$ through the interval $\Delta\theta$ and above $\bar{\theta}$. Unfortunately, no measurements through such high T have been found in the literature; but relevant c_{ij} vs. T of single crystals are known.

(c) Fig. 2 displays two features of critical importance in the analysis to follow. With two exceptions at $\ln T < 0.5$, the data points at $\ln T < 1.4$ scatter randomly in the narrow band between Martin's -13.199 for single crystals and -13.189 for polycrystals, and the latter matches Wycherley's [16] value for polycrystalline aggregates. The zero slope around which all of the 17 points average confirms the value of $\gamma/3R = 0.00002795$ as consistent with $\bar{\theta}(0) = 220.5$ K. Wycherly's γ, reported to only three significant figures, led to systematic positive deviations from the best value as indicated by the dashed line in Fig. 2 at $\ln T < 0.6$. The best values of γ and $\bar{\theta}(0)$ in combination are consistent with $(C_V - \gamma T)/3RT^3 = 10.1061[\bar{\theta}(0)]^{-3} = \text{const}$ at all $T < \bar{\theta}(0)/50$ where, in this case, $\bar{\theta}(0) = 220.5$ when $\gamma/3R = 0.00002795$.

The second feature to be noted is that the maximum dispersion is not at $\ln T_m \equiv 3.547 = \ln 0.1573\bar{\theta}(0)$, as it would be in an isotropic solid, but at a slightly lower $\ln T_m, \approx 3.4$. This shows that the formulas, $\bar{\theta}(0) = [3/(\gamma^3 + 2)]^{1/3}\theta_l$, $(\gamma = \theta_t/\theta_l)$, derived for isotropic solids by Barber and Martin [1] do not hold for polycrystalline copper although the aggregate is macroscopically isotropic in acoustic wave velocities due to random orientations of its crystalline components. Hence, conventional methods of averaging the three longitudinal moduli and six transverse moduli of single crystals over all orientations to find the one effective bulk modulus κ_L and two equal rigidity moduli, G_L, of the aggregate are not appropriate for Eq. (12) in Ref. [1] which is derived to represent all differing moduli separately, regardless of their number or their differences. It would be pointless, therefore, to obscure the differences by conventional methods of averaging although, as will be shown, alternative ways of averaging can be applied to reduce the number of

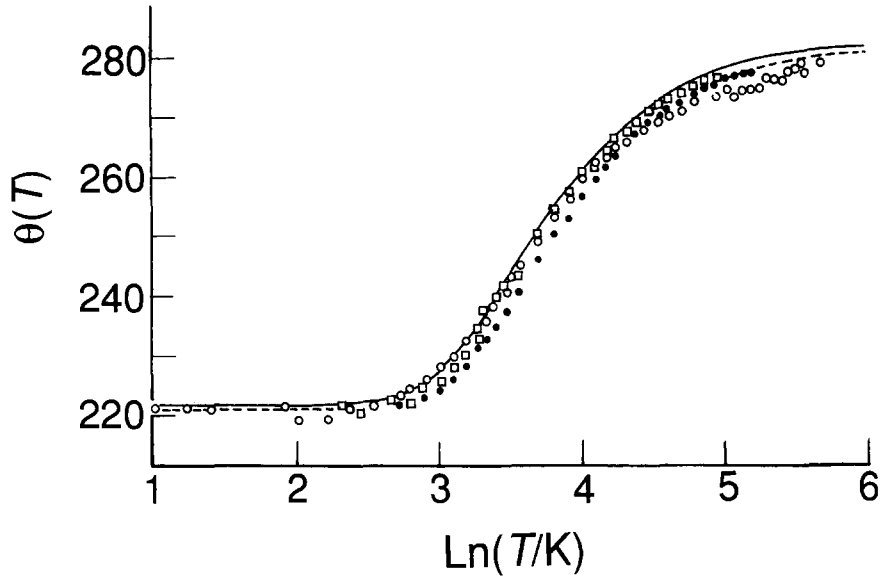

Fig. 3. $\theta(T)$ for single crystal copper. —selected curve for single crystal copper (strain free); the strained single crystal with $g(\theta_{te}) = 1/3g(\theta_t)$ by ○; the same with $(\theta_{te}) = 1/4g(\theta_t)$ by □; experimental polycrystal by •. $|\bar{\theta}(0)\,\mathrm{K}, \bar{\theta}(T)\,\mathrm{K}, \Delta\theta\,\mathrm{K}|$ for strain free; |221.7, 283.6, 61.9| for strained crystals by ○: |220.7, 282.8, 62.1| for strained crystals by □; |220.7, 282.8, 62.1| for experimental polycrystals; |220.5, ~280, ~60|.

terms in Eq. (12) [1] to three or more (but not less than three).

Considerations (a), (b), and (c) imply that single crystals, which may require from 9 to 18 terms in Eq. (12) of Ref. [1], must be understood before polycrystalline aggregates can be adequately represented as functions of c_{ij}. To do this, the required c_{ij}, s_{ij} and formulas relating them to Eq. (12) of [1] are represented in Table 1 and Fig. 3.

3.2. *Elastic constants and acoustic mode distributions in single crystal and polycrystalline copper*

The elastic constants c_{ij} and s_{ij} of single crystals and the several conventional averages of them, representing bulk (κ) and rigidity (G) moduli, are from a comprehensive Handbook by Simmons and Wang [22].

Three sets of parallel plane waves account for nine distributions of acoustic modes in cubic crystals. As shown in de Launay's review [7], these are functions of c_{ij} in single crystals, where they are defined by three sets of Miller indices: (100), (110), (111). Nine separate values of $\theta_l(100)$, $\theta_l(110)$, $\theta_l(111)$, $\theta_{t1}(100)=\theta_{t2}(100)$, $\theta_{t1}(110)$, $\theta_{t2}(110)$, $\theta_l(111) = \theta_{t2}(111)$ are defined in copper by the general equation

$$\theta(\mathrm{lmn}) = [\mathrm{h}/(k\pi a\rho^{1/2})]\left(\sum c_{\mathrm{ij}}\right)^{1/2} = 277.85\left(\sum c_{ij}\right)^{1/2}$$

When, according to de Launay, the bulk modulus of electron gas, $\kappa_e = c_{12} - c_{44}$, is added to each lattice bulk modulus, κ_L; three higher values of $\theta_l(\mathrm{lmn})$ are defined:

ij	11	12	44	$\kappa_e = c_{12} - c_{44}$
c 10^{12} dyn cm^{-2}	1.7620	1.2494	0.8177	6.4317
s 10^{12} dyn cm^{-2}	1.3788	0.5720	1.2229	

c_{ij} and s_{ij} at $T = 0$, density = 9.0305 g cm^{-3}.

$$\theta_e(\mathrm{lmn}) = h(k\pi a\rho^{1/2})(\kappa_L + \kappa_e)^{1/2}$$
$$= 277.85(\kappa_L + \kappa_e)^{1/2}$$

In anisotropic crystals constrained toward more isotropic symmetries by pressures from contiguous crystals in polycrystalline copper, three equal values of θ_t must be considered, one for each set of Miller indices:

$$\theta_e(\mathrm{lmn}) = h(\pi a\rho^{1/2})(\kappa_e) = 277.85\,\kappa_e^{1/2}$$

Thus a total of $9\theta(\mathrm{lmn}) + 3\theta_{le}(\mathrm{lmn}) + 3\theta_e(\mathrm{lmn})$ must be considered to determine $\theta(0)$ according to the equation

$$\bar{\theta}(0) = \left[1/\mathrm{n}\sum_{\mathrm{n=1}}^{\mathrm{m}} 1/\theta_n^3(\mathrm{lmn})\right]^{-1/3}$$

where n = 9 if $\kappa_e = 0$ and n = 18 if $\kappa_e > 0$.

* Note: Sets of $\theta_l(\mathrm{lmn})$, $\theta_{le}(\mathrm{lmn})$, $\theta_e(\mathrm{lmn})$ must be considered separately and the ratios $\theta_l : \theta_{t1} : \theta_{t2}$ must be defined for each θ_l.

The high temperature limit of $\bar{\theta}(1)$, defined by $\bar{\theta}(T) = [\Pi\theta_n(\mathrm{lmn})]^{1/n}(4/\pi)^{1/3}$ requires the T-dependence of all 18 $\bar{\theta}(\mathrm{lmn})$. These are implicit in tables of c_{ij} vs. T by Simmons and Wang [22] and the following equations are inferred from plots of $\bar{\theta}(\mathrm{lmn})$ vs. T. Because the plots are not exactly linear for $T < 100$ K, the values at $T = 0$ are listed independently to show how they differ from intercepts linear in T.

3.3. Determination of $\bar{\theta}(0)$ as a Function of c_{ij}

The most critical parameter of Eq. (12) of Ref. [1] is the effective mean of all relevant θ_l, θ_{le}, θ_{t1}, θ_{t2}, θ_e at $T = 0$ as listed in Table 2. At such low temperatures, all acoustic waves are mutually independent and velocity dispersion is zero for all $\theta = h\nu^*/k$. Then, the effective mean is defined by the arithmetic mean of reciprocals cubed as defined in the equation $\theta(0) = \left[1/n\sum_n(1/\theta_n^3(\mathrm{lmn})\right]^{-1/3}$.

The next most critical parameter of Eq. (12) in Ref. [1] is the high-temperature limit of $\bar{\theta}(T)$. This is defined in Section 3.2 as the geometric mean of all the T-dependent θ's involved. In strain-free single crystals, these two means apply to all θ's listed in Table 2, *except* θ_e which does not combine with any transverse plane waves. In strained polycrystals, θ_e couples with some but not all transverse modes, and the degree of coupling depends on obscure variables such as dimensions of polycrystals, degree of strain in them, and magnitude of $\kappa_e = c_{12} - c_{44}$. These effects can be assessed empirically by finding what combinations of θ's account for the experimental values of $\bar{\theta}(0)$ and $\bar{\bar{\theta}}(4/\pi)^{1/3}$ as labeled in Fig. 1.

The problem of inferring appropriate means for the θ's from the several combinations of eighteen or more possible values is most conveniently understood from a two-dimensional array in which three sets of parallel plane waves are represented in columns and intersecting combinations of planes are represented in rows. Arithmetic means of each column and geometric means of each row should thus be most appropriate in effective total means, $\bar{\theta}(0)$ and $\bar{\bar{\theta}}$, respectively.

Table 3 presents such an array with the several arithmetic and geometric means and defines the several combinations that must be considered.

The array of 3 columns and 4 rows excluding θ_e in Table 3 represents the sum of two 3×3 arrays in which θ_{t1} and θ_{t2} rows are identical while θ_l is specified in one array and θ_{le} in the other. Both arrays represent a single crystal in which the deforming strain is zero; i.e. $(c_{12} - c_{14})$ is in equilibrium with deviations from spherical symmetry imposed by the anisotropy of the lattice. In such a crystal, according to de Launay [7], κ_e of the electron gas is added to the bulk modulus of the lattice, κ_L, making the effective modulus $(\kappa_L + \kappa_e) > \kappa_L$ and $\theta_{le} > \theta_l$ in each set of parallel plane waves, as shown. Although de Launay considered only the higher modulus, the lower one must also be considered here, because the lattice modes can persist in a homogeneous isotropic atmosphere of electrons at any nominal pressure.

The combination of modes expected in a large single crystal is characterized by the values of $\bar{\theta}(0)$ and $\bar{\bar{\theta}}\theta_e$ line (a). The $\bar{\bar{\theta}}(0) = 215.0$ is 6.4 K lower than Martin's value for single crystal copper, 221.4, indicating that $[\sum(1/\theta^3)/n]^{-1/3}$ is not appropriate for all 18 modes. The geometric means of each row averaged by this formula yields $\bar{\theta} = 228.4\,\mathrm{K} > 221.4\,\mathrm{K}$ by 7 K. This higher value is expected in nonparallel plane waves defined by three different sets of Miller indices interacting by coupling on mutual intersecting lines, while the parallel plane waves in each set do not. The results indicate that the arithmetic mean of these two extremes, $(215.0 \pm 228.4)/2 = 221.6$ K do match the

Table 3
Calculation of $\theta(0)$ and $\theta(T)$ for plausible combinations of θ_l, θ_{t1}, θ_{t2}, and θ_e in crystalline copper [a]

θ	Miller indices				$\theta(0,\|\|)$	θ	θ_e
(K)	g(θ)	(100)	(110)	(111)	(K)	(K)	(K)
θ_l || Plane waves	1	368.9	423.5	440.2	406.2	409.7	409.7
θ_{le} || Plane waves	1	411.5	442.8	452.7	434.2	435.4	435.3
θ_{t1} || Plane waves	2	251.3	251.3	185.0	219.4	221.9	226.9
θ_{t2} || Plane waves	2	251.3	140.7	185.0	172.9		187.0
θ_e Deformation waves	2	182.6	182.6	182.6			182.6
$\bar{\theta}(0)$					215.0	228.4	225.0
$\underline{\bar{\theta}}(0) = (1/2)(\theta(0,\|\|) + \theta(0) =$						221.7	220.0
$\underline{\bar{\theta}} = (\theta_t \cdot \theta_l \cdot \theta_{t1}^2 \cdot \theta_{t2}^2)^{1/6} =$						261.7	259.6
$\bar{\theta}(4/\pi)^{1/3}$						183.6	281.4
$\Delta\theta = \bar{\theta} - \theta(0)$						62.1	61.4
$\bar{\theta}(0)$ if g(θ_l) = 0 and g(θ_{le}) = **2**					215.4	228.7	225.4

[a] The numbers in this array are for $T = 0$ from Table 2. $\theta(0)$ is a function of those only while θ is, in principle, the geometric mean of the same θ's at $T > \theta_l$ according to Eqs. (5.6) through (5.20). With one exception, coefficients of T in these formulas are small and decrease in significance as parameters of C_V as T increases above ≈200 K. In these preliminary calculations they have been neglected because the one exception, $\theta_e(T)$ increases with T so as to compensate those that decrease and make their means nearly independent of T.
Modes that involve κ_e are distinguished (by subscript 'e') from those that do not because we wish to decide whether they couple or combine so as to obscure some lattice modes or not.

experimental 221.4 K, as it should in accord with the very plausible assumption that there are as many coupled states as there are parallel states.

3.4. Tentative conclusion

In single crystals free of deforming strain, $\bar{\theta}(0) = [(\bar{\theta}(0)\|) + \bar{\theta}(\bar{\theta}')]/2$, where $\bar{\theta}(0)$ represents parallel waves, $\bar{\theta}'$ represents intersecting plane waves, for equal number densities of each.

Item (b) in Table 3 is identical to (a) except that all θ_l are changed to θ_{le}. This increases both $\bar{\theta}(0)$ and $\underline{\bar{\theta}}$; but the increases are so trivial that they neither confirm nor refute co-existence of $\theta_l < \theta_{le}$. They only show how insensitive $\bar{\theta}(0)$ and $\underline{\bar{\theta}}$ are to changes in θ_l, representing only 1/6 of the modes. Both are much more sensitive to changes in θ_t, representing 1/3 to 2/3 of the modes.

The column headed $\bar{\theta}(\theta_e)$ (implying transverse modes are functions of θ_e) represents single crystals in shape-changing strain as in polycrystalline aggregates. Such conditions generate deformation modes characterized by $\theta_e = 182.6$ K in copper. This is essentially equivalent to transverse modes in the (111) planes, $\theta_t(111) = 185.0$ K but is not to be identified with them because it vanishes when $\kappa_e \to 0$ while transverse modes do not. It differs from them in that it is independent of direction while transverse modes vary with direction between 251.3 and 140.7 K. Hypothetically, it should approximate the effective mean of transverse modes in isotropic polycrystalline aggregates as function of strain-constants s_{ij}. This is given by $277.85\ G_R^{1/2} = 183.5$ K, where G_R at $T = 0$ is 0.436×10^{12} dyn cm^{-2} in tables calculated by Simmons and Wang [22]. The approximation to 182.6 K is remarkable and elucidating when the reasons for it are understood.

To understand why $\theta_e(0)$ approximates a mean of transverse modes in polycrystalline copper, alternative ways of averaging over the c_{ij} and s_{ij} of single crystals are to be considered.

3.5. Mean values of θ_l, θ_{le}, θ_t in isotropic polycrystalline copper

Simmons and Wang [22] list values of bulk modulus, κ, and rigidity modulus, G, for polycrystalline copper at $T = 0$ as shown in Table 4.

The lines V, H, S, R are effective averages of single crystal c_{ij} and s_{ij} according to Voight (c_{ij}) [23] Hashin [24], Shtrikman [25], and Reuss (s_{ij}) [26]. In the literature, there is uncertainty about which, if any, of the four values of G is reliable, but there is a general consensus that $G_V = 0.593$ and $G_R = 0.436$ are limit-

Table 4
Bulk and rigidity moduli for polycrystalline copper

Author	$10^{17}\,\kappa$ (N cm^{-2})	10^{12} G (N cm^{-2})	$\theta_K = \bar{\theta}_l$ (K)	$\theta_G = \bar{\theta}_t$ (K)	$\bar{\theta}(0)$ (K)
V(23)	1.420	0.593	331.1	214.0	
H(24)	1.420	0.537	331.1	203.6	
S(25)	1.420	0.500	331.1	196.5	
R(26)	1.420	0.436	331.1	183.5	
(V+R)/2	1.420	0.5145	331.1	199.3	220.4

ing values between which certainty must be found. These limits as defined by Simmons and Wang are:

$$G_\nu = (c_{11} - c_{12} + 3c_{44})/5,$$
$$G_R = (4s_{11} - 4s_{12} + 3s_{44})^{-1}/5$$

Anderson [27] proposed the arithmetic mean of these two values as most appropriate, with this estimate being confirmed by $\bar{\theta}(0) = \{[(1/\theta_\kappa^3) + (2/\theta_G^3)]/3\}^{-1/3} = 220.4$ K in remarkable accord with Martin's experimental value for polycrystalline copper, 220.7 K, and Wycherley's 220.5 K. But the corresponding $\bar{\bar{\theta}}(4/\pi)^{1/3} \equiv [\theta_\kappa \theta_G^2 (4/\pi)]^{1/3} = 255.8$ K is much too small (compared to 280 K to reproduce the experimental $\bar{\theta}(T)$ vs. T. Furthermore, no reasonable combination of the six θ_t's in Table 3 yields a mean value of 199.3. None of these averaging schemes can work without adding κ_e to κ_v on each of the three axes to yield

$$\theta_l v_e = (1.420 + 3 \times 0.4317)^{1/2} - 277.85$$
$$= 457.8\,\text{K}$$

This approximates $\theta_{le}(111) = 452.7$, but $\theta_t = 199.3$ must be lowered to 195.1 if $\bar{\theta}(0)$ is to remain at 220.5 K.

Evidently no reasonable combination of the Voight and Reuss [23,26] parameters can reproduce $\bar{\theta}(T)$ vs. T of polycrystals, because they do not account for deformation modes related to κ_e in small crystals in deforming stress fields of contiguous crystals. However, these values, being functions of observed elastic constants, must be significant in the heat capacity of polycrystalline copper. Since $\theta_e = 182.6$ K occurs in both polycrystals and single crystals, subject to deforming external forces, and since θ_G (in strain)=183.5 K and $\theta_t(111) = 185.0$ K are so similar, these three values can be interchanged in any of the plausible combinations without significantly changing the values of $\bar{\theta}(0)$ or $\bar{\bar{\theta}}$ in them. These substitutions alone justify combinations of parameters from both single crystals and isotropic polycrystals to represent polycrystalline aggregates. Furthermore, it shows that other substitutions can improve conformance of Eq. (12) in Ref. [1] with experimental data, if they are compatible with experimental limits $\bar{\theta}$ and $\bar{\bar{\theta}}(4/\pi)^{1/3}$.

3.6. Calculation of $\bar{\theta}(T)$ vs. T for predictable combinations of acoustic mode density distributions

Table 3 contains all of the parameters required to represent the following predictable status of copper if (as justified earlier) the temperature dependence of elastic constants c_{ij} is neglected:

1. Single crystals free of shape-changing strain but constrained to constant volume against internal pressure of valence electron gas.
2. Single crystals assisting shape-changing stress from external forces while constrained to constant volume as in a polycrystalline aggregate at $T \ll T_{melt}$.

Different combinations of arithmetic and geometric averaging over different combinations of parameters are required for cases (1) and (2).

Case (1)

Parameters : θ_l/K : 368.9(1)*, 423.5(1), 440.2(1)
θ_{le}/T : 411.5(1), 442.8(1), 452.7(1)
θ_{t1}/T : 215.3(2), 215.3(2), 185.0(2)
θ_{t2}/T : 215.3(2), 140.7(2), 185.0(2)

* (n)=number of terms having this value of θ.

As shown in Table 3,

$$\bar{\theta}(0)\text{according to Section 3.5} = 221.7$$
$$\bar{\bar{\theta}}(T) \equiv \theta(r/\pi)^{1/3} = \underline{2}83.6$$
$$\Delta\theta = 62.1$$

$\theta(T)$ vs. ln T, according to [1] with these parameters, is represented in Fig. 2 by the solid line. Agreement with experimental points (○) is remarkable at $\ln T < 3.55$ corresponding to $T < 35$ K, very similar to $T_m = 0.1573, \bar{\theta} = 34.9$ K. At $\ln T > 3.55$, the experimental points fall farther below as ln T increases to 5.3 ($T = 200$ and at higher temperatures the (○) points are increasingly scattered and uncertain.

Case (2):

Parameters: Identical with those in (1) except that two levels of deformation strain are represented:

(a) by substituting $\theta_e = 182.6(4)$ K for $\theta_t(111) = 185.0(4)$ K because these values, differing by only 2.4 K, lead to $\bar{\theta}(0) = 220.7$ K in exact accord with the experimental value, 220.5 K;
(b) by substituting $\theta_e = 182.6(3)$ K for three values of θ_{t2}, namely 251.3, 140.7, and 185 K because the effective mean of this row, $(172.9 + 187)/2 = 180.0$ K, is 2.6 K lower than θ_e and 5 K lower than $\theta_t(111)$ indicating that (b) is more probable than (a).

Other reasons for preferring (b) are that it represents a lower average of deforming strain – three terms instead of four in (a) – and a more even distribution of strain – three dimensions compared to one (111) in (a).

The average level and distribution of deforming strain in polycrystalline copper depends on the size and orientations of crystals and is, therefore, unknown; but assumptions (a) and (b) represented by (□) and (•), respectively, in Fig. 3 show the expected trends toward lower $\bar{\theta}(0)$. Between $\ln T = 3.5$ and 4.5, the experimental points (○) drift from the solid lines toward the (□) points. The further lowering of experimental points as ln T increases above 4.5 indicates that values of θ_l and θ_{le} are depressed to lower effective means in polycrystalline aggregates. Small effects of this kind may be due to the small decreases of c_{ij} with increasing T as shown in Eq. (5.1) through Eq. (5.12) in [Table 2]. These are neglected in Fig. 3 because they appear to be fully compensated by increases in θ_e vs. T as indicated in Eq. (5.13) through Eq. (5.15) [in Table 2].

Whatever causes the lower than expected values of $\bar{\theta}(T)$ between $\ln T = 4.6$ and ≈5.4, they are well represented by a simpler combination of effective means from Table 3. Evidently the coupling of all modes as $\ln T \rightarrow \ln\bar{\theta}(0) = 5.4$, as labeled in Fig. 4, levels all terms in Table 3 to the effective means of each row. This suggests that the means of each row can be used as parameters in Eq. (12) of Ref. [1].

3.7. Combinations of θ, θ_{le}, θ_{tl}, θ_{t2}

Several combinations of mean values from Table 3 are plausible. Maximum levels of deformation strain associated with severe anisotropy of copper may be best represented by only six terms from four rows in Table 3:

$$\bar{\theta}_l \equiv \frac{406.2 + 409.7\,\text{K}}{2} = 408.0(1)\,\text{K}$$
$$\bar{\theta}_{le} = \frac{434.2 + 435.3\,\text{K}}{2} = 434.8\,\text{K}$$
$$\bar{\theta}_{tl} \equiv \frac{219.4 + 226.9\,\text{K}}{2} = 223.2(2)\,\text{K};$$
$$\theta_e = 182.6(2)\,\text{K}$$
$$\bar{\theta}(0) = 222.2\,\text{K}; \quad \Delta\theta = 57.8\,\text{K};$$
$$\bar{\bar{\theta}}(4/\pi)^{1/3} = 280\,\text{K}$$

$\bar{\theta}(T)$ vs. ln T as function of these parameters is shown in Fig. 5. The agreement with experimental points is the most that can be expected from such averaging at all T's represented. The largest deviations from experimental values are between $\ln T = 3.0$ and ≈3.7, where calculated values of $\bar{\theta}(T)$ are lower than experimental values. This is due to loss of the lowest $\theta_{t2}(= 140.7\,\text{K})$ in the mean. $\bar{\theta}_{t2} \equiv (172.9 + 187)/2\,(1/2)\text{K} = 180\,\text{K}$ which is replaced here by $\bar{\theta}_e = 182.6$ K. Had $\bar{\theta}_{t2} = 180$ K been used instead of $\bar{\theta}_e = 182.6$ K, this part of the curve would have been shifted about −0.01 K toward lower T and provided slightly better accord with experiment. But $\theta(0)$ would have been reduced from 222.2 to 221.8 and this would make the calculated points slightly lower than in Fig. 4. The points at $\ln T >\sim 4$ would not be changed significantly because $\Delta\theta$ would be increased to about 58.2 K.

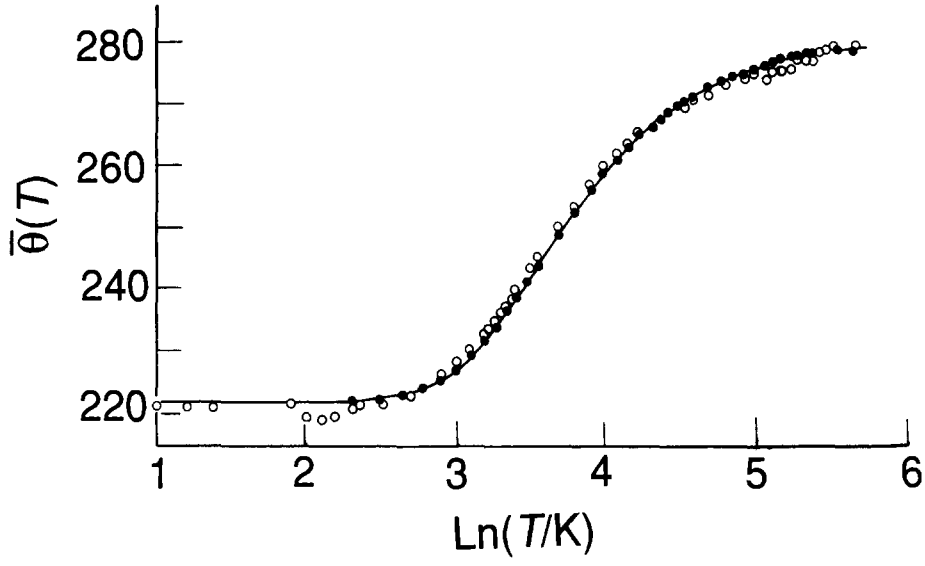

Fig. 4. $\theta(T)$ for polycrystalline copper. Selected curve for polycrystalline copper (strained) ———; Eq. (12) [1] values $\theta_l(0) = 406.2(1)$ K; $\theta_{le}(0) = 434.2(1)$ K; t(0) = 219.4(2) $\bar{\theta}_e = 182.6(2)$; $\theta(0) = 222.2$; $\Delta\theta = 57.8$ and $\bar{\bar{\theta}}(4/\pi)^{1/3} = 280$ K. • – calculated values; and ○ – experimental points.

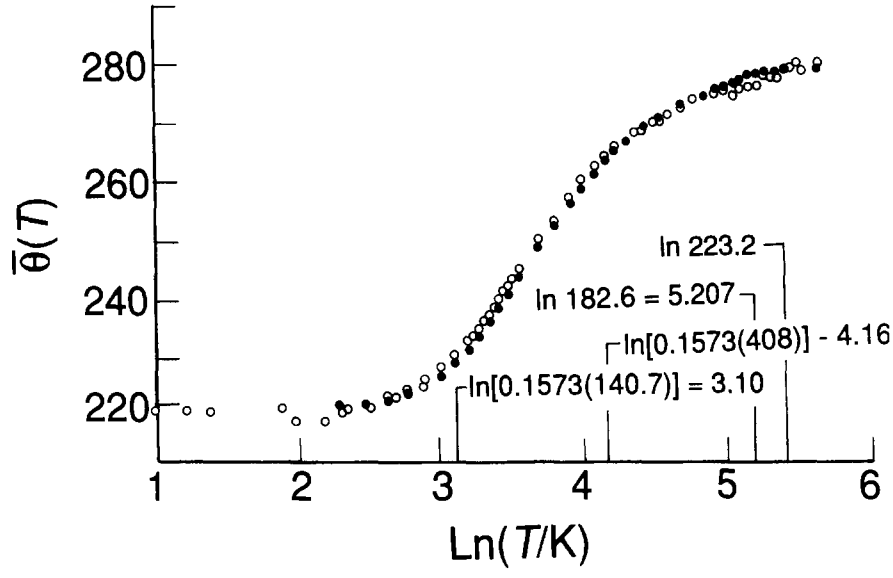

Fig. 5. $\bar{\theta}(T)$ for polycrystalline copper; six terms in Eq. (12) [1]. $\bar{\theta}_l(0) = (406.2 + 409.7)/2 = 408.0$ K(1 term); $\bar{\theta}_{le}(0) = 434.2 + 435.3)/2 = 434.8$ K(1 term); $\bar{\theta}_{t1} = (219.4 + 226.9)/2 = 232.2(2)$; $\bar{\theta}_{t2} = 182.692)$; $\bar{\theta}(0) = 222$; $\bar{\bar{\theta}}(4/\pi)^{1/3} = 280$; $\Delta\theta = 57.8$. • – theoretical; and ○ – experimental.

The effect of averaging out $\theta_{t2}(111) = 140.7$ K is best seen in Fig. 6 where the ratio, C_V(calc)/C_V(exptl), is plotted as a function of ln T. The maximum deviation from the reference line, $C_V(\text{calc})/C_V(\text{exptl}) = 1.00$, is at ln T corresponding to the lowest $\theta_{t2}(111) = 140.7$ K in single crystals – the temperature at which Eq. (12) of Ref. [1] for single crystals conforms most exactly to experimental data.

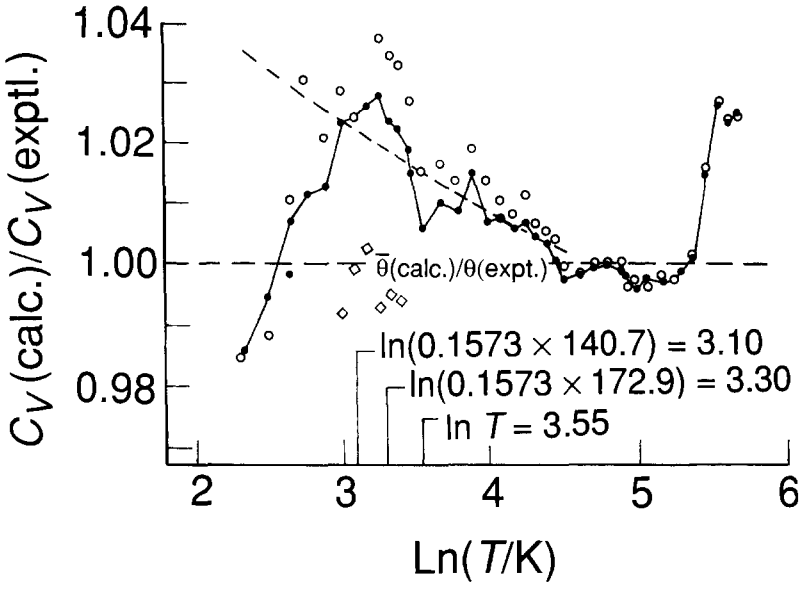

Fig. 6. Calculated C_V ratio for copper for six and three terms.

The points (•) for six terms in Fig. 6 simply show what accuracy is lost by averaging out the lowest frequencies in the crystals. The loss is only about 2% of C_V and less than 1% of $\bar{\theta}(0)$, when six terms are averaged.

It is interesting now to consider what accuracy is lost by averaging to only three terms (i.e., assuming perfect isotropy) in polycrystalline copper. This is done by choosing

$$\theta_l \equiv (408.0 + 434.8)/2 = 421.4(1)\,\mathrm{K}$$

$$\theta_t \equiv (223.2 + 182.6)/2 = 202.9(2)\,\mathrm{K}$$

These values imply $\bar{\theta}(0) = 228.1\,\mathrm{K}$ and $\bar{\theta}(4/\pi)^{1/3} = 280.6\,\mathrm{K}$. The latter remains in excellent accord with experiment, but $\bar{\theta}(0) = 228.1\,\mathrm{K}$ is unacceptably high. A better value would be found if $\bar{\theta}_{t2} \equiv (223.2 + 172.9)/2 = 198.0\,\mathrm{K}$ is assumed. Then $\bar{\theta}(0) = 222.9\,\mathrm{K}$ in exact accord with the six-term averages. This corresponds to assigning only half as many transverse modes to $\bar{\theta}_e = 182.6\,\mathrm{K}$ – a choice allowed because it depends on unknown sizes of crystalline components.

The points representing three-term averages in Fig. 6 were calculated from the same values of $\bar{\theta}(0)$ and $\Delta\theta$ as were the six-term averages. This allows most meaningful comparisons with the six-term points. The (○) points, representing complete isotropy, are higher than the (•) points by about 1%. Thus, inaccuracies of the three-term function are only about 3% at their low-temperature maximum. This is still a very useful approximation when – as is often true – accurate values of c_{ij} are not available.

The calculations presented here for copper exemplify the complications and inaccuracies arising from anisotropies in single crystals created by polycrystalline aggregates even where these anisotropies are only partially obscured by the macroscopic isotropy of aggregates. The greatest difficulties occur in determinations of the limiting values of $\theta(T), \bar{\theta}(0)$, and $\Delta\theta(T) = \bar{\theta}(4/\pi)^{1/3} - \bar{\theta}(0)$. If these are known, the T-dependence of C_V is represented well by Eq. (12) of Ref. [1] even when its parameters are averaged to only 3 terms corresponding to perfect isotropy of randomly oriented anisotropic crystals in strongly bound aggregates.

These conclusions and considerations are also critically relevant to glass-forming crystals and the glasses made from them.

Acknowledgements

Until his recent premature death in 1988, Stephen W. Barber devoted his retirement years coaching me

and my students on the calculational aspects of this work, and this preview suggests the nature of what is to be achieved once the entire endeavor can be presented. The work and the analysis are entirely based on his 1959 paper with Steve Martin [1].

References

[1] S.W. Barber and B. Martin, J. Phys. Chem. Solids, (1959) 198.

[2] P. Debye, Zur Theorie der spezifischen Wärmen, Ann. Phys. Leipzig 39, (1912) 789. (Translated into English in Collected Papers of P.J.W. Debye, Interscience, New York, 1954).

[3] E. Schrödinger, Handbuch der Physik, Springer, Berlin, X (1926) p. 325.

[4] S.W. Kieffer, Revs. Geophys. Space Phys., 17 (1979) 20, 35..

[5] L. Brillouin, Wave Propagation in Periodic Structures, Dover, New York (1953) pp. 255.

[6] M. Blackman, The Specific Heat of Solids in Handbuch der Physik, Springer, New York, 7 (1) (1942) p. 325.

[7] J. de Launay, The Theory of Specific Heats and Lattice Vibrations, in Solid State Physics, F. Seitz and D. Turnbull (Eds.), 2 (1956) pp. 219–303.

[8] M. Born and T. von Kármán, Theory of Specific Heat, Phys. Z., 14 (1913) 15.

[9] V.V. Tarassov, New Problems in the Physics of Glass (translated from the Russian edition of 1959). The English edition produced by the OTS, Jerusalem, for U.S. Dept. of Commerce, Washington, DC (1963).

[10] M. Dank and S.W. Barber, J. Chem. Phys., 23 (1955) 5.

[11] V.V. Tarassov, Phys. Stat. Solidi, 20 (1967) 37.

[12] S.W. Kieffer, Heat capacity and entropy: Systematic relations to lattice vibrations, in S.W. Kieffer and A. Navrotsky (Eds.), Reviews in Mineralogy, Microscoptic to Macroscopic, Mineralogical Society of America, Blacksburg, VA (1985) p. 65.

[13] N. Komada and E.F. Westrum Jr., Phonon Dispersion, J. Chem. Thermodyn., 29 (1997) 311.

[14] N. Komada, Scapolites, J. Chem. Thermodyn., 28 (1996).

[15] N. Komada and E.F. Westrum Jr.B.S. Hemingway and L.M. Anovitz, J. Chem. Thermodyn., 27 (1995) 1097.

[16] K.E. Wycherley, Dissertation, but cf. Leadbetter and K.E. Wycherley, J. Chem. Thermodyn., 2 (1970) 855.

[17] T.C. Cetus, C.R. Tilford and C.A. Swenson, Phys. Rev., 174 (1968) 835.

[18] D.L. Martin, Phys. Rev., B 7 (1972) 5357.

[19] D.L. Martin, Can. J. Phys., 47 (1969) 1253.

[20] D.L. Martin, Can. J. Phys., 38 (1960) 17.

[21] N.E. Phillips, Low temperature heat capacity of metals in Crit. Rev. Solid State Science, CRC, NY, 2 (1971) 467.

[22] G. Simmons and H. Wang, Single Crystal Elastic Constants, and Calculated Aggregate Properties: A Handbook, 2nd ed., MIT Press, MA (1971).

[23] W. Voight, Lehrbuch der Krystallphysik, Teubner, Leipzig (1928).

[24] Z. Hashin and S. Shtrikman, J. Mech. Phys. Solids, 10 (1962) 335.

[25] S. Shtrikman, J. Mech. Phys. Solids, 10 (1962) 343.

[26] A. Reuss, Z. Angew. Math. Mech., 9 (1929) 49.

[27] O.L. Anderson, in W.P. Mason (Ed.), Physical Acoustics, Academic Press, III, B (1965) 347.